

Three-dimensional mixing in Stokes flow: the partitioned pipe mixer problem revisited

V.V. Meleshko^a, O.S. Galaktionov^{a,b}, G.W.M. Peters^{b,*}, H.E.H. Meijer^b

^a *Institute of Hydromechanics, National Academy of Sciences, 252057 Kiev, Ukraine*

^b *Dutch Polymer Institute, Eindhoven Polymer Laboratories, Eindhoven University of Technology, P.O. Box 513, 5600 MB Eindhoven, The Netherlands*

(Received 24 April 1998; revised 22 February 1999; accepted 7 March 1999)

Abstract – The velocity field and mixing behaviour in the so-called partitioned pipe mixer were studied. Starting with the same physical model as in previous studies, an exact analytical solution was developed which yields a more accurate description of the flow than the previously used approximate solution. Also, the results are in better accordance with the reported experimental data. © 1999 Éditions scientifiques et médicales Elsevier SAS

Stokes flow / laminar distributive mixing / static mixers

1. Introduction

The aim of the present paper is to study the three-dimensional creeping flow in an infinitely long cylindrical pipe with internal walls, that divide the pipe into a sequence of semicircular ducts. Such a system, called the ‘partitioned pipe mixer’ (PPM) was introduced by Khakhar et al. [1] as a prototype model for the widely used Kenics static mixer (Middleman [2]).

In the Kenics mixer each element is a helix, twisted on a 180°, plate; elements are arranged axially within a cylindrical tube so that the leading edge of an element is at right angles to the trailing edge of the previous one. Computational fluid dynamics tools make a straightforward numerical simulation of this kind of three-dimensional flow feasible (Avalosse and Crochet [3], Hobbs and Muzzio [4], Hobbs et al. [5]). However, such simulations do require significant computational resources, especially when studying the effect of varying parameters on the mixing process. Therefore, simplified analytical models, that give the possibility of fast simulations of the process (or mimic its features closely enough), are still useful.

The PPM model of the essentially three-dimensional flow was highly idealized, nevertheless retaining the main features of the flow under study. The model involves two superimposed, independent, two-dimensional flow fields: a cross-sectional (rotational) velocity field and a fully developed axial Poiseuille profile in every semicircular duct. This gives two independent two-dimensional boundary problems instead of the three-dimensional problem. The solution proposed by Khakhar et al. [1] for the cross-sectional velocity field was only an approximate one. There exists, however, ‘exact’ analytical solutions in a closed form.

In the present paper we use these exact solutions to examine the mixing properties in this three-dimensional mixer. Important differences in some mixing patterns were obtained, and our results resemble more closely the available experimental results of Kusch and Ottino [6].

* Correspondence and reprints: Department of Mechanical Engineering, Building W.h. 0.119, Eindhoven University of Technology, P.O. Box 513, 5600 MB Eindhoven, The Netherlands; e-mail: gerrit@wfw.wtb.tue.nl

2. Velocity field in PPM

Consider the interior of an infinite cylinder $0 \leq r \leq a$, $0 \leq \theta \leq 2\pi$, $|z| < \infty$, which contains inside a sequence of rigid rectangular plates of length L (see, for example, figure 6.2 in Ottino [7]). Neighbouring plates are placed orthogonally to each other, namely $0 \leq r \leq a$, $\theta = 0, \pi$, $2kL \leq z \leq (2k+1)L$ and $0 \leq r \leq a$, $\theta = \pi/2, 3\pi/2$, $(2k+1)L \leq z \leq (2k+2)L$, where $k = 0, \pm 1, \pm 2, \dots$. The flow in all semicircular ducts is induced by a constant pressure gradient $\partial p/\partial z$ and the uniform rotation of the cylindrical wall $r = a$ with constant velocity V ; the inner walls remain fixed. Following Khakhar et al. [1], we assume that the axial velocity profile is fully developed in every cross-section (neglecting transition effects between two plates) and cross-sectional velocities v_r and v_θ are such as they would be in case of an infinitely long semicircular duct. In the Stokes approximation the steady velocity field with components v_r , v_θ and v_z is defined from two uncoupled independent solutions of the two-dimensional problems

$$\Delta \Delta \psi = 0, \quad (1)$$

$$\mu \Delta v_z = -\frac{\partial p}{\partial z} \quad (2)$$

in each of the semi-circular domains. Here, Δ stands for the Laplace operator in polar coordinates, μ is the fluid viscosity, and $\psi(r, \theta)$ represents the stream function of the cross-sectional flow with

$$v_r = \frac{1}{r} \frac{\partial \psi}{\partial \theta}, \quad v_\theta = -\frac{\partial \psi}{\partial r}. \quad (3)$$

In what follows we consider the ‘basic’ domain $0 \leq r \leq a$, $0 \leq \theta \leq \pi$, $0 \leq z \leq L$; the solutions for other domains can be obtained straightforwardly from this basic one. The no-slip boundary conditions in terms of ψ and v_z are

$$\begin{aligned} \psi = 0, \quad \frac{\partial \psi}{\partial r} = -V \quad \text{for } r = a, \quad 0 \leq \theta \leq \pi, \\ \psi = 0, \quad \frac{\partial \psi}{\partial r} = 0 \quad \text{for } 0 \leq r \leq a, \quad \theta = 0, \pi \end{aligned} \quad (4)$$

and

$$\begin{aligned} v_z = 0 \quad \text{for } r = a, \quad 0 \leq \theta \leq \pi, \\ v_z = 0 \quad \text{for } 0 \leq r \leq a, \quad \theta = 0, \pi, \end{aligned} \quad (5)$$

for Eqs (1) and (2), respectively.

The biharmonic problem (1), (4) admits an exact analytical solution:

$$\psi = \frac{2V}{4 - \pi^2} \left(\pi r \sin \theta - \frac{\pi(a^2 - r^2) + 4ar \sin \theta}{2a} \arctan \frac{2ar \sin \theta}{a^2 - r^2} \right), \quad (6)$$

which can be obtained in the following way.

Let us introduce the bipolar coordinates (ξ, η) such that the two poles of the coordinates are located on the x -axes at the points $(\pm a, 0)$:

$$x + iy = ai \cot \frac{\xi + i\eta}{2}. \quad (7)$$

Then

$$x = r \cos \theta = J \sinh \eta, \quad y = r \sin \theta = J \sin \xi, \tag{8}$$

where $a/J = \cosh \eta - \cos \xi$, and the quantity $1/J$ is the first Lamé differential parameter of this orthogonal coordinate system. This system for the two-dimensional biharmonic equation was firstly used in Joukowski [8]; see Joukowski and Chaplygin [9] for the exact solution of the problem for the Stokes flow between eccentric cylinders.

The semicircle $0 \leq r \leq a$, $0 \leq \theta \leq \pi$ in polar coordinates transforms into the strip $-\infty \leq \eta \leq \infty$, $\pi/2 \leq \xi \leq \pi$ in bipolar coordinates. The biharmonic equation (1), which must be satisfied by the stream function ψ , in bipolar coordinates is written as

$$\left(\frac{\partial^4}{\partial \xi^4} + 2 \frac{\partial^4}{\partial \xi^2 \eta^2} + \frac{\partial^4}{\partial \eta^4} + 2 \frac{\partial^2}{\partial \xi^2} - 2 \frac{\partial^2}{\partial \eta^2} + 1 \right) \Psi = 0 \tag{9}$$

for the auxiliary function $\Psi = \psi/J$.

By means of the equality

$$\frac{\partial \Psi}{\partial \xi} = \frac{1}{J} \frac{\partial \psi}{\partial \xi} + \psi \frac{\partial(1/J)}{\partial \xi} = \frac{\partial \psi}{\partial n_\xi} + \psi \frac{\sin \xi}{a}, \tag{10}$$

(where n_ξ denotes the outer normal to the line $\xi = \text{constant}$) we can reformulate the boundary conditions (3) in terms of Ψ as

$$\begin{aligned} \Psi = 0, \quad \frac{\partial \Psi}{\partial \xi} = 0 \quad \text{at } \xi = \frac{1}{2}\pi, \quad |\eta| \leq \infty, \\ \Psi = 0, \quad \frac{\partial \Psi}{\partial \xi} = V \quad \text{at } \xi = \pi, \quad |\eta| \leq \infty. \end{aligned} \tag{11}$$

By choosing a solution of Eq. (9),

$$\Psi = A \sin \xi + B \cos \xi + C \xi \sin \xi + D \xi \cos \xi, \tag{12}$$

we can satisfy all boundary conditions (11), provided that the values of the constants A, B, C, D are

$$A = \frac{2\pi}{\pi^2 - 4} V, \quad B = -\frac{2\pi^2}{\pi^2 - 4} V, \quad C = -\frac{4}{\pi^2 - 4} V, \quad D = \frac{2\pi}{\pi^2 - 4} V. \tag{13}$$

Returning from $\Psi(\xi)$ in (12) to the stream function $\psi(r, \theta)$ by means of equalities

$$J \sin \xi = r \sin \theta, \quad J \cos \xi = \frac{r^2 - a^2}{2a}, \quad \xi = \pi - \arctan \frac{2ar \sin \theta}{a^2 - r^2}, \tag{14}$$

after some reductions, we come to expression (6).

The behaviour of the stream function ψ near the corner point $(a, 0)$ can be obtained from the expansion of expression (6) into a Taylor series in the local polar coordinates (ρ, χ) with $x = a - \rho \sin \chi$, $y = \rho \cos \chi$. The first term linear in ρ is

$$\psi_{\text{loc}} = -\frac{4V\rho}{\pi^2 - 4} \left(\chi \cos \chi + \frac{1}{2}\pi \chi \sin \chi - \frac{\pi^2}{4} \sin \chi \right), \tag{15}$$

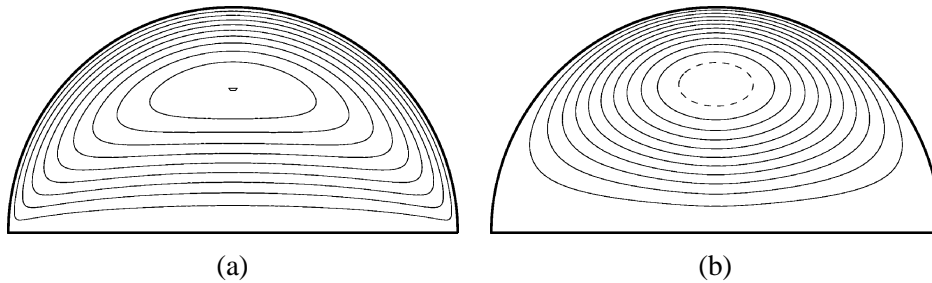


Figure 1. Streamline patterns (contour plot of stream function) of (a) analytical solution (6) and (b) one-term approximate solution (16). Contour lines are equidistant with the same step in both plots. Dashed line in (b) represents the contour, which is absent in (a).

which corresponds to the ‘scraping’ solution (Goodier [10], Taylor [11]) for a quarter plane $\rho \geq 0$, $0 \leq \chi \leq \pi/2$ with the constant tangential velocity $-V$ applied at the plane $\chi = 0$.

Figure 1(a) shows contour levels of the stream function (6). The cross-sectional flow exhibits a single vortex cell with one elliptic stagnation point at $(0.636a, \pi/2)$.

The previous studies (Khakhar et al. [1], Ottino [7]) suggested the approximate one-term solution of the boundary problem (1), (4):

$$\Psi^* = \frac{4Va}{3\gamma} \left(\frac{r}{a}\right)^2 \left\{ 1 - \left(\frac{r}{a}\right)^\gamma \right\} \sin^2 \theta, \quad \gamma = (11/3)^{1/2} - 1 \approx 0.915, \quad (16)$$

which has been obtained by a variational method. This expression (16), however, does not satisfy both the governing biharmonic equation (1) and the no-slip condition at the moving boundary! It turns out that the tangential velocity at the boundary $r = a$ varies as $(4/3)V \sin^2 \theta$ instead of being constant V . Therefore, the velocity is overestimated (up to 33% at the circular boundary) in some zones far from the flat boundary, and it is artificially smoothed near corners. The contour plot of the stream function according to one-term solution (16) is presented in figure 1(b).

The solution of boundary problem (2), (5) for the fully developed axial flow in a semicircular duct reads (Ottino [7]):

$$v_z = \frac{16\pi}{\pi^2 - 8} \langle v_z \rangle \sum_{k=1}^{\infty} \left\{ \left(\frac{r}{a}\right)^{2k-1} - \left(\frac{r}{a}\right)^2 \right\} \frac{\sin[(2k-1)\theta]}{(2k-1)\{4 - (2k-1)^2\}}, \quad (17)$$

where

$$\langle v_z \rangle = \frac{8 - \pi^2}{4\pi^2} \frac{1}{\mu} \frac{\partial p}{\partial z} a^2$$

is the average axial velocity. Using straightforward transformations and tables of infinite sums (Prudnikov et al. [12]), we can present expression (17) in a closed form:

$$v_z = \frac{2\pi}{\pi^2 - 8} \langle v_z \rangle \left\{ -\pi \frac{r^2}{a^2} \sin^2 \theta + \left(\frac{r}{a} - \frac{a}{r}\right) \sin \theta - \frac{1}{4} \left(\frac{r^2}{a^2} - \frac{a^2}{r^2}\right) \sin(2\theta) \right. \\ \left. \times \ln \frac{r^2 + 2ar \cos \theta + a^2}{r^2 - 2ar \cos \theta + a^2} + \frac{1}{2} \left[2 - \left(\frac{r^2}{a^2} - \frac{a^2}{r^2}\right) \cos(2\theta) \right] \arctan \frac{2ar \sin \theta}{a^2 - r^2} \right\}, \quad (18)$$

which is preferable for numerical simulations of the advection process. It is worth mentioning that the first three terms of the infinite sum (17) used in Khakhar et al. [1] and Ottino [7] provide reasonable accuracy with

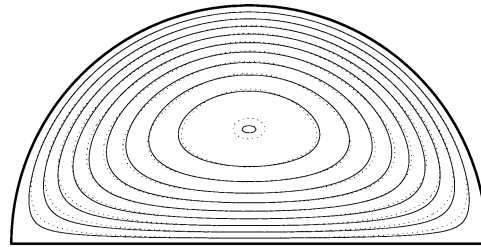


Figure 2. Contour plots of the axial velocity v_z : solid lines correspond to the exact expression (18), dotted lines correspond to three-terms approximation of (17).

maximum errors (compared to ‘exact’ expression (18)) that are within a few percent. In *figure 2* the contour lines of v_z , defined by (18) are shown as a solid lines, while the same contours for three-term approximation of (17) are plotted as dotted lines. Despite this approximation the shape of the contours is rather similar, the discrepancy amounts up to 7% of the average velocity $\langle v_z \rangle$, reaching a maximum not far from the corner points, where the velocity v_z is underestimated. Increasing the number of terms in (17) to one hundred, reduces the relative error to less than 0.005%, but, it will take much more computer time to simulate the passive tracers advection.

3. Chaotic mixing in PPM

The motion of a passive individual (Lagrangian) particle is described by the advection equations

$$\frac{dr}{dt} = v_r(r, \phi), \quad r \frac{d\theta}{dt} = v_\theta(r, \phi), \quad \frac{dz}{dt} = v_z(r, \phi), \tag{19}$$

with the velocity field on the right hand side of (19) defined by (6) and (18). The initial conditions are $r = r_0, \theta = \theta_0, z = 0$ at $t = 0$.

Here the variable ϕ is obviously defined as

$$\phi = \begin{cases} \theta, & 2kL \leq z < (2k + 1)L, \quad 0 \leq \theta \leq \pi, \\ \theta - \pi, & 2kL \leq z < (2k + 1)L, \quad \pi < \theta < 2\pi, \\ \theta - \pi/2, & (2k + 1)L \leq z < (2k + 2)L, \quad \pi/2 \leq \theta \leq 3\pi/2, \\ \theta + \pi/2, & (2k + 1)L \leq z < (2k + 2)L, \quad 0 \leq \theta < \pi/2, \\ \theta - 3\pi/2, & (2k + 1)L \leq z < (2k + 2)L, \quad 3\pi/2 < \theta < 2\pi, \end{cases} \tag{20}$$

where $k = 0, \pm 1, \pm 2, \dots$

System (19) describes a steady motion of an individual particle along the streamline in each compartment. However, as the flow is three-dimensional and spatially periodic, it can exhibit chaotic behaviour (Aref [13, Section 5.4]).

In Khakhar et al. [1] the single non-dimensional parameter β , the ‘mixing strength’

$$\beta = \frac{4VL}{3\gamma \langle v_z \rangle a}, \tag{21}$$

was introduced to completely describe the behaviour of such a system. Although the parameter γ has no particular meaning for the exact solution (6), the value of β is used to compare our results with those of the literature.

Poincaré mapping was applied to reveal the zones of regular and chaotic motion. The Poincaré maps were constructed by taking an initial point (r_0, θ_0) at the level $z = 0$ and recording the coordinates of the intersections of the trajectory with the planes $z_n = 2nL$, $n = 0, \pm 1, \pm 2, \dots$

The Poincaré maps for several values of β were computed and analysed using both the approximate and exact solution. Here we present the resulting Poincaré maps for which one single starting point was chosen in the chaotic zone (*figure 3*). White regions in the plots correspond to islands. The boundaries of the islands are plotted as thin solid lines.

Islands in Poincaré maps correspond to the Kolmogorov–Arnold–Moser (KAM) tubes in the flow. The fluid captured in such a tube will only travel inside, not mixing with the rest of the fluid outside the tube. The influence of the KAM tube on mixing can be characterized by the relative flux carried by the tube compared to the total flux through the mixer. So, for the islands both their area and the flux carried by corresponding KAM tubes are evaluated. The flux can be computed as the integral of v_z over the islands area, or, by using Stokes theorem, as a contour integral over the boundary of islands.

Figures 3(a) and *3(b)* present the Poincaré maps for $\beta = 4$. For the approximate solution the eight largest islands are clearly seen (*figure 3(a)*). They occupy about 49% of the cross-section area and carry approximately 55% of the total flux. The exact solution provides a completely different system of islands (*figure 3(b)*). Their influence is considerably lower since they occupy only about 13% of the area and bear 18% of the total flux.

The difference becomes even stronger for larger values of the mixing strength β . *Figures 3(c)* and *3(d)* represent the case of $\beta = 8$. The approximate solution provides two large islands that occupy about 13% of the cross-section (see *figure 3(c)*) and bear 18% of total flux, while the islands revealed by the exact solution (*figure 3(d)*) occupy only about 0.7% of the cross-section area. The relative flux through KAM tubes amounts in this case to approximately only 1% of total flux.

In both examples presented the total area of the cross-section of the KAM tubes is significantly smaller when the exact solution is used. As both the approximate and exact solutions are based on the same simplified model of the PPM, i.e. neglecting the transition effects at the joints of the mixer elements, the calculated shape of the KAM tubes should be considered with some reservations. The relative cross section of, and the relative flux through these tubes are of more relevance and they can give a useful estimation of these values for practical flows.

Streaklines can serve as a tool to characterise the mixing and to visualise underlying mixing mechanisms. Kusch and Ottino [6] noted that computed streaklines, originating from a cross-section of a KAM tube, are much different from those experimentally observed. Computed streaklines for $\beta = 8.0$ and the experimental results obtained for $\beta = 10.0 \pm 0.3$ were compared to get, at least, some resemblance. They pointed out that the PPM model can hardly mimic closely the experimental results (due to the small length of dividing plates—less than the pipe radius). However, the results of numerical simulations using the corrected velocity field (6), (18) and the right value for β gives a much better agreement. *Figures 3(e)* and *3(f)* show the Poincaré maps for $\beta = 10$, using both solutions. In *figure 3(f)* the approximate contours of the two islands of period 2 are plotted with solid lines. These contours were used to reveal the shape of the correspondent KAM tubes (see *figure 4(c)*). Contours were represented by closed polygons and the vertices of these polygons were then tracked numerically through four mixing elements, showing the outer boundary of the KAM tube. The other two images in *figure 4* represent the numerical (*a*) and experimental (*b*) results from Kusch and Ottino [6], respectively. As for the experimental results the actual value of mixing strength was $\beta = 10.0 \pm 0.3$, we calculated the KAM tube

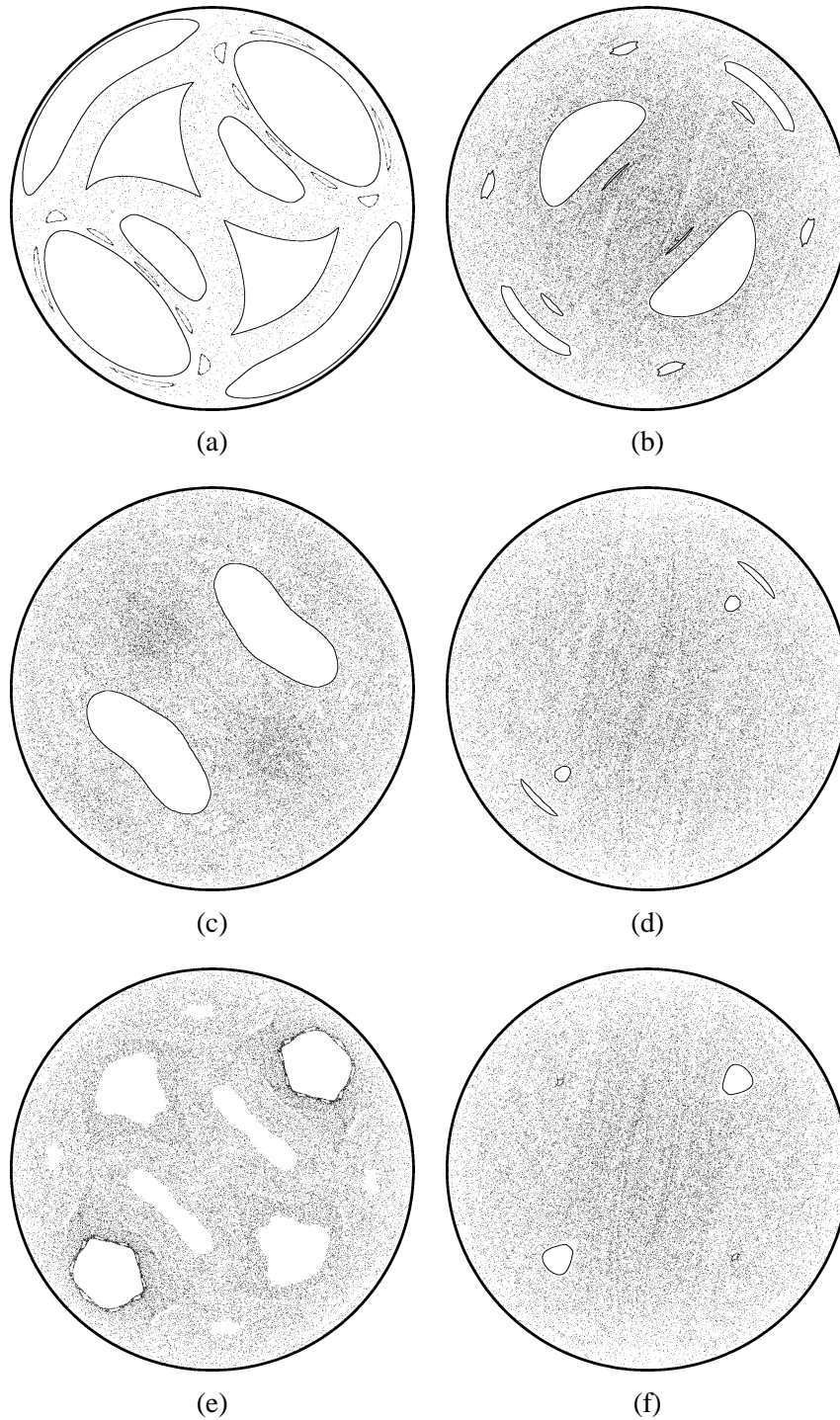


Figure 3. Poincaré maps for different values of mixing strength $\beta = 4$ ((a) and (b)), $\beta = 8$ ((c) and (d)), $\beta = 10$ ((e) and (f)), respectively. Pictures in the left column ((a), (c), (e)) were obtained by using approximate solution (16), (17), while those in the right column were obtained by using the exact solution (6), (18).

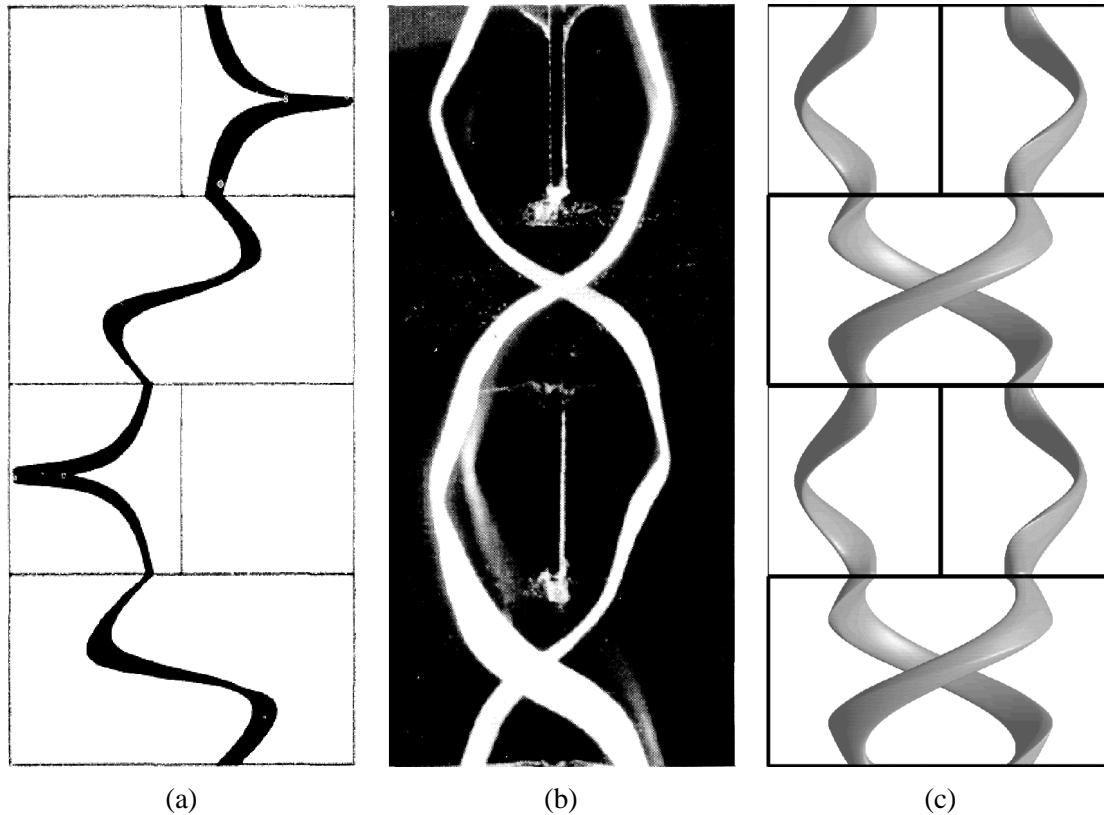


Figure 4. Computed KAM tubes for the PPM model with mixing strength parameter $\beta = 10.0$ (c) compared with (a) computed ($\beta = 8$) and (b) experimental ($\beta = 10.0 \pm 0.3$) streaklines from Kusch and Ottino [6]. (Images (a) and (b) are taken from figure 9 of the cited paper, reproduced with permission from Cambridge University Press.)

shapes for the limiting values $\beta = 9.7$ and $\beta = 10.3$ as well. The overall shape of the tubes does not change much, variation of mixing strength influences mainly the tube thickness: it is thinner for larger β parameter and vice versa.

Kusch and Ottino [6] did not specify explicitly the location where the dye for streakline visualization was injected. However, it is easy to show that when the dye is injected just a little outside the KAM tube, this is clearly visible because the dye starts to spread over the mixing elements. To illustrate this, circles were drawn around the geometrical center of the island (see *figure 3(f)*). Markers were evenly distributed on the boundary of every circle and tracked through four mixing elements (two spatial periods) of the PPM. In *figure 5(a)* the radius of the circle was $0.03a$, thus all markers were positioned well inside the KAM tube. In *figure 5(b)* the circle (of radius $0.062a$) touches the tube boundary. Such streaklines can be slightly deformed but are still captured completely within the tubes. In *figure 5(c)* the initial circle was slightly larger than the island shown in *figure 3(f)*, and thus contains markers outside the KAM tube. It is clearly seen that within just four mixing cells the markers spread over the whole cross-section of the pipe.

The use of approximate numerical solution (16), (17) led Kusch and Ottino [6] to a great discrepancy with experimental results for $10 < \beta < 40$: experiments showed remarkably stable KAM tubes, while computations exhibited a lot of bifurcations (see, for example, *figure 10(d)* from their paper). However, using the exact solution (6), (18) relatively simple stable structures are predicted. For example, for a relatively large mixing strength of $\beta = 20$, four KAM tubes of first order were found but no KAM tubes of period 2 were detected.

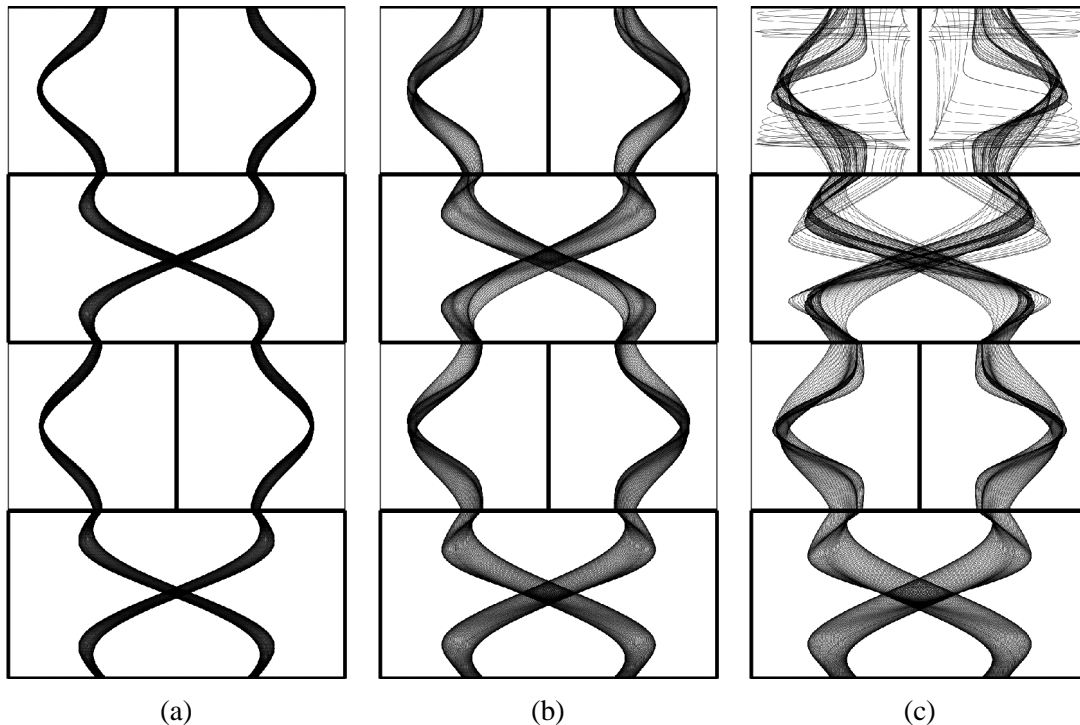


Figure 5. Traces of the markers, originally regularly spaced on circles of different radii, centered around the geometrical centers of the islands of period 2. Each circle contains 100 markers. The radii are: (a) $0.03a$ —well inside the KAM tube, (b) $0.062a$ —touching its boundary, (c) $0.08a$ —circumscribing the tube boundary.

The cross section of these tubes (and, consequently, the flux associated with them) is relatively small. These periodical structures are, nevertheless, stable.

4. Conclusions

Although the flow under study is merely a prototype flow, it possesses some important features of flows in widely used mixing devices. The comparison of an approximate and an exact solution, obtained within the framework of the same model, shows the possible major consequences of some mathematical simplifications. Such simplifications can cause large differences in the predicted systems' behaviour, especially for systems that are supposed to exhibit chaotic properties. Here, the difference in the predicted behaviour was caused by the use (in previous studies) of a one-term approximate solution that artificially smoothes the cross-sectional velocity field. The exact solution shows much better agreement with the reported experimental results.

Of course, there exists an important problem regarding the abrupt transition between mixing elements and ignoring developing flows at these transitions. Results of recent numerical simulations (Hobbs et al. [5]) show that, indeed, this is a major assumption: for the Kenics mixer with a finite thickness of helical screwed mixing plates, flow transitions at the abrupt entrance and exit of each element strongly affect the velocity field over up to one quarter of the element length.

However, the conclusion from the results presented of the importance of an accurate description of the velocity field in mixing flows, where even small changes can significantly alter the overall mixing behaviour of the system, is still applicable for real industrial situations.

Acknowledgements

The authors would like to acknowledge support by the Dutch Foundation of Technology (STW), grant no. EWT44.3453. We also thank one of the referees for expressing the opinion that unenlightened use of the computer or uninformed parametrizations can lead one to nonsensical results.

References

- [1] Khakhar D.V., Franjione J.G., Ottino J.M., A case study of chaotic mixing in deterministic flows: the partitioned pipe mixer, *Chem. Eng. Sci.* 42 (1987) 2909–2919.
- [2] Middleman S., *Fundamentals of Polymer Processing*, McGraw-Hill, New York, 1977.
- [3] Avalosse T., Crochet M.J., Finite element simulation of mixing: 2. Three-dimensional flow through a Kenics mixer, *AICHE J.* 43 (1997) 588–597.
- [4] Hobbs D.M., Muzzio F.J., Effects of injection location, flow ratio and geometry on Kenics mixer performance, *AICHE J.* 43 (1997) 3121–3132.
- [5] Hobbs D.M., Swanson P.D., Muzzio F.J., Numerical characterization of low Reynolds number flow in the Kenics static mixer, *Chem. Eng. Sci.* 53 (1998) 1565–1584.
- [6] Kusch H.A., Ottino J.M., Experiments on mixing in continuous chaotic flows, *J. Fluid Mech.* 236 (1992) 319–348.
- [7] Ottino J.M., *The Kinematics of Mixing: Stretching, Chaos and Transport*, Cambridge University Press, Cambridge, 1989.
- [8] Joukowski N.E., Motion of a viscous fluid contained between rotating eccentric cylindrical surfaces, *Proc. Khar'kov Math. Soc.* 1 (1887) 34–37 (in Russian). German abstract: *Jb Fortschr. Math.* 19 (1887) 1019.
- [9] Joukowski N.E., Chaplygin S.A., Friction of a lubricated layer between a shaft and its bearing, *Trudy Otd. Fiz. Nauk Obshch. Lyub. Estest.* 13 (1904) 24–36 (in Russian). German abstract: *Jb Fortschr. Math.* 35 (1904) 767.
- [10] Goodier J.N., An analogy between the slow motion of a viscous fluid in two dimensions, and systems of plane stress, *Philos. Mag. Ser. 7* 17 (1934) 554–564.
- [11] Taylor G.I., On scraping viscous fluid from a plane surface, in: Schäfer M. (Ed.), *Miszellangen der Angewandten Mechanik (Festschrift Walter Tollmien)*, Akademie-Verlag, Berlin, 1962.
- [12] Prudnikov A.P., Brychkov Yu.A., Marichev, O.I., *Integrals and Series*, Vol. 1, Gordon and Breach, London, 1986.
- [13] Aref H., Stirring by chaotic advection, *J. Fluid Mech.* 143 (1984) 1–21.